

**TRANSVERSE ENERGY DISTRIBUTIONS IN NUCLEUS-NUCLEUS COLLISIONS  
IN THE DUAL MONTE CARLO MULTI-CHAIN FRAGMENTATION MODEL**

J. Ranft\*  
CERN, Geneva

**ABSTRACT**

Particle production in nucleus-nucleus collisions is calculated in a Monte Carlo version of the dual multi-chain fragmentation model. The model uses an efficient method to sample the numbers of interactions in nucleus-nucleus collisions. We calculate distributions in the transverse energy and multiplicity and compare with data obtained at the CERN SPS in O-Pb collisions with 200 GeV per nucleon.

To be published in Physics Letters B

---

\* Permanent address:

Sektion Physik, Karl-Marx-Universität, Leipzig, GDR

High energy collisions of heavy ions offer the exciting possibility to discover experimentally a new state of matter, the quark-gluon plasma [1].

Experimental studies using nuclei accelerated up to 200 GeV per nucleon started in 1986 at the CERN SPS and first experimental results have been presented [2].

In order to understand what signatures of heavy ion collisions point to the formation of a quark-gluon plasma, we should, however, also study such collisions within conventional models of low  $P_{\perp}$  particle production. Such conventional events are the background against which the effects of the quark-gluon plasma have to be found.

A first version of the Monte Carlo dual multistring fragmentation model was studied by Möhring, Ranft and Ritter [3]. This model was based on the formulation of Capella et al. [4]. The model was also used by Capella et al. [5] to calculate the leading baryon spectrum in heavy ion collisions.

The distribution function for the number of inelastic collisions  $n$ , in which  $n_A$  ( $n_B$ ) nucleons of the nuclei  $A$  ( $B$ ) participate, in the formulation given in [4] was not well suited to sample  $n$ ,  $n_A$  and  $n_B$  in a Monte Carlo calculation. Therefore in [3], especially for heavy nuclei, the distribution from which  $n$ ,  $n_A$  and  $n_B$  were sampled, had to be approximated.

An efficient as well as elegant method for the Monte Carlo sampling of  $n$ ,  $n_A$  and  $n_B$  in high energy collisions of the nuclei  $A$  and  $B$  was recently described by a Dubna group [6]. We use this method in the new present version of the Monte Carlo dual multistring fragmentation model. For the fragmentation of the quark-antiquark and quark-diquark strings into hadrons the code BAMJET [7] is used. The same code is used extensively for sampling hadron-hadron and hadron-nucleus collisions [8,9] in the dual multistring fragmentation model.

In Fig. 1 we give an example for the chain structure of the dual multistring fragmentation model for collisions of the nuclei  $A$  and  $B$ .

In a nucleus-nucleus collision with  $n$  inelastic interactions in which  $n_A(n_B)$  nucleons participate, there are  $2n$  hadronic chains formed.

For  $n_B > n_A$  one has

$2n_A$  valence-valence chains  $(qq)_B - q_B$  and  $(qq)_B - q_A$ ,  
 $2(n_B - n_A)$  valence-sea chains  $(qq)_B - q_A^s$  and  $q_B - \bar{q}_A^s$ , and  
 $2(n - n_B)$  sea-sea chains  $\bar{q}_B^s - q_A^s$  and  $q_B^s - \bar{q}_A^s$ .

The average number of collisions  $n$  and participating nucleons  $n_A$  and  $n_B$  (examples are given in Table 1) depends only weakly on the collision energy. However, at low collision energy the invariant masses of many sea-sea chains are below the masses of the mesons which could be formed out of the quarks at the end of the strings. The kinematics at low collision energy forces the suppression of many sea-sea chains. In order to keep energy and momentum conservation, their energy and momentum is given to the valence-valence and valence-sea chains.

In Fig. 2 we give for oxygen-nucleus and sulfur-nucleus collisions the distribution of the number of nucleons from the projectile nuclei O and S  $n_O(n_S)$ , which take part in the collision. For light target nuclei, we find one maximum in the distributions for  $n_O(n_S)$  equal to one. This is the case of peripheral nucleus-nucleus collisions at large impact parameters. For heavy target nuclei, a second maximum rises at  $n_O = 16$  and  $n_S = 32$ . This corresponds to the case of central collisions.

In Table 2 we give average multiplicities obtained from the model for O-A and S-A collisions at different energies. We give the total multiplicities  $\langle n_{tot} \rangle$ , the charged multiplicities  $\langle n_{ch} \rangle$  and the multiplicities of protons  $\langle n_p \rangle$  and neutrons  $\langle n_n \rangle$ . These multiplicities refer to the average collisions. In central collisions still higher multiplicities are obtained [3]. The proton and neutron multiplicities refer to high energy nucleons from the fragmentation of the chains. Protons and neutrons resulting from the subsequent breakup of the remaining nuclear fragments are not included.

In Fig. 3 we present the distribution of the total transverse energy

$$E_{\perp} = \sum_i \sqrt{m_i^2 + p_{\perp i}^2}$$

calculated for oxygen collisions with Al, Cu, Sn and Au nuclei. We present the  $E_{\perp}$  distributions for all secondaries as well as for the charged secondaries alone. The distributions were obtained using 2000 sampled events in each case. We found also [10] a strong correlation between the total transverse energy and the highest central energy density obtained in the nucleus-nucleus collisions.

In a paper presenting first experimental results on oxygen-lead collisions, the NA-35 Collaboration at the CERN SPS [2] gives the transverse energy distribution in a central rapidity region. In Fig. 4 we compare the distribution obtained from our model with the data [2].

We include in our plot all particles with lab-rapidities  $2.2 < y < 3.8$  and transverse momenta  $P_{\perp}$  (in GeV/c)  $> -0.05 + 0.05$  y. For secondary protons and neutrons, which are not identified in the experiment, we use  $P_{\perp}$  instead of  $E_{\perp}$ . The actual acceptance of the detector in the experiment [2] has a more complicated shape and differs slightly for different secondaries. Therefore it is possible that we accept too many secondaries in the calculation, overestimating the total  $E_{\perp}$ .

We find the general shape of the calculated distribution in Fig. 4 in rough agreement with the experimental distribution. The striking feature of both distributions is the peak at large  $E_{\perp}$ . This peak corresponds to central collisions. The tail of the calculated distribution extends to slightly larger  $E_{\perp}$  than found in the experiment.

The model is rather well defined and has only few parameters which could be adjusted to the experimental data. Some fine tuning of the distribution might be possible by changing the scattering amplitude, which is used as input for the  $n$ ,  $n_A$  and  $n_B$  distribution and by changing the prescription for the kinematic suppression of

chains with small invariant mass. Fermi-momentum could be introduced for the nucleons in the colliding nuclei and intrinsic transverse momenta could be introduced for the quarks and diquarks at the end of the chain.

In a subsequent paper [10] we will present the model and the results obtained in more detail. Here we conclude from this first comparison to experimental data that the dual multistring fragmentation model given a remarkable agreement with the experimental data of these collisions in a completely new energy range.

#### ACKNOWLEDGEMENT

The author thanks H.J. Möhring and S. Ritter, who collaborated in the first version of this model. He acknowledges useful discussions with Dr. S.Yu. Shmakov, who also provided him with a FORTRAN program for sampling from the distribution of Ref. [6]. He would like to thank Dr. K. Goebel for the hospitality in his group at CERN, where this paper was completed.

# REFERENCES

1. E.V. Shuryak, Phys. Rep. 61, 71 (1980);  
M. Jacob and H. Satz, eds. Quark matter formation and heavy ion collisions. Proc. of Bielefeld Workshop, May 1982, Singapore, World Scientific, 1982;  
R. Hagedorn, preprint CERN-TH 3684 (1983).
2. A. Bamberger et al., NA-35 Collaboration, preprint CERN/EP 86-194 (1986).
3. H.J. Möhring, J. Ranft and S. Ritter, Z. Phys. C 27, 419 (1985).
4. A. Capella, C. Pajares and A.V. Ramallo, Nucl. Phys. B 241, 75 (1984).
5. A. Capella, A.V. Ramallo, J. Tran Thanh Van, J.A. Casado and C. Pajdres, Orsay preprint LPHE 86-10 (1986).
6. A.M. Sadoroshnii, W.W. Ushinskii and S.Yu. Shmakov, Dubna preprint P2-86-361 (1986).
7. J. Ranft and S. Ritter, Acta Phys. Pol. B 11, 259 (1980);  
S. Ritter, Comp. Phys. Commun. 31, 393 (1984).
8. J. Ranft and S. Ritter, Z. Phys. C 20, 347 (1983; Z. Phys. C 27, 413 (1985); Z. Phys. C 27, 569 (1985).
9. P. Aurenche, F.W. Bopp and J. Ranft, Z. Phys. C 23, 67 (1984);  
Phys. Rev. D 33, 1867 (1986).
10. J. Ranft, to be published elsewhere.

Table 1

Average number of interactions  
in nucleus-nucleus collisions

A	B	$N_A$	$N_B$	$N_{tot}$
O	Al	5.6	6.6	10.4
O	Cu	6.7	10.4	16.1
O	Sn	7.9	14.8	23.2
O	Pb	8.6	20.7	32.0
O	Au	8.6	20.2	31.7
S	Al	9.7	8.8	15.2
S	Cu	11.8	15.7	27.1
S	Sn	13.7	23.3	40.5
S	Pb	14.6	29.7	51.5

Table 2

Average multiplicities of secondary particles in nucleus-nucleus collisions according to the dual multichain fragmentation model

A	B	E GeV/N	$\langle n_{\text{tot}} \rangle$	$\langle n_{\text{ch}} \rangle$	$\langle n_p \rangle$	$\langle n_n \rangle$
O	Al	60	67	37.4	5.5	5.6
		200	103	59	5.8	5.8
		1000	152	89	6.1	6.2
O	Cu	60	101	56	8.2	8.4
		200	146	84	8.0	8.1
		1000	228	133	8.7	9.0
O	Sn	60	113	63	9.3	9.9
		200	195	112	10.4	10.7
		1000	294	171	10.8	11.3
O	Pb	1000	410	237	14.9	15.7
		200	244	138	12.8	13.8
		100	178	99	12.0	13.0
		50	123	67	11.3	12.2
		20	51	27.2	7.9	8.4
		10	39	19.7	8.1	8.7
		5	31	15.4	7.8	8.4
O	Au	60	138	76	11.7	12.6
		200	246	140	13.0	13.9
S	Al	200	155	89	8.8	9.0
		1000	235	137	9.7	9.4
S	Cu	200	245	140	12.9	13.2
		1000	356	207	13.3	13.7
S	Sn	200	332	190	16.8	17.6
		1000	516	300	18.4	19.5
S	Pb	200	394	224	19.8	21.1
		1000	646	375	22.4	23.1



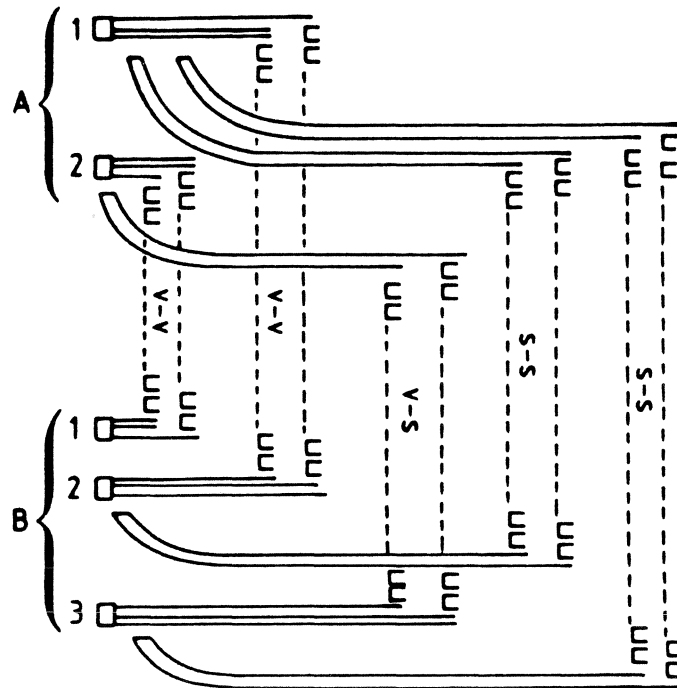


Fig. 1. Example of a nucleus-nucleus scattering process with  $n = 5$  interactions and  $n_A = 2$  contributing nucleons from nucleus A and  $n_B = 3$  contributing nucleons from nucleus B. This gives rise to 4 valence-valence chains, 2 valence-sea chains and 4 sea-sea chains.

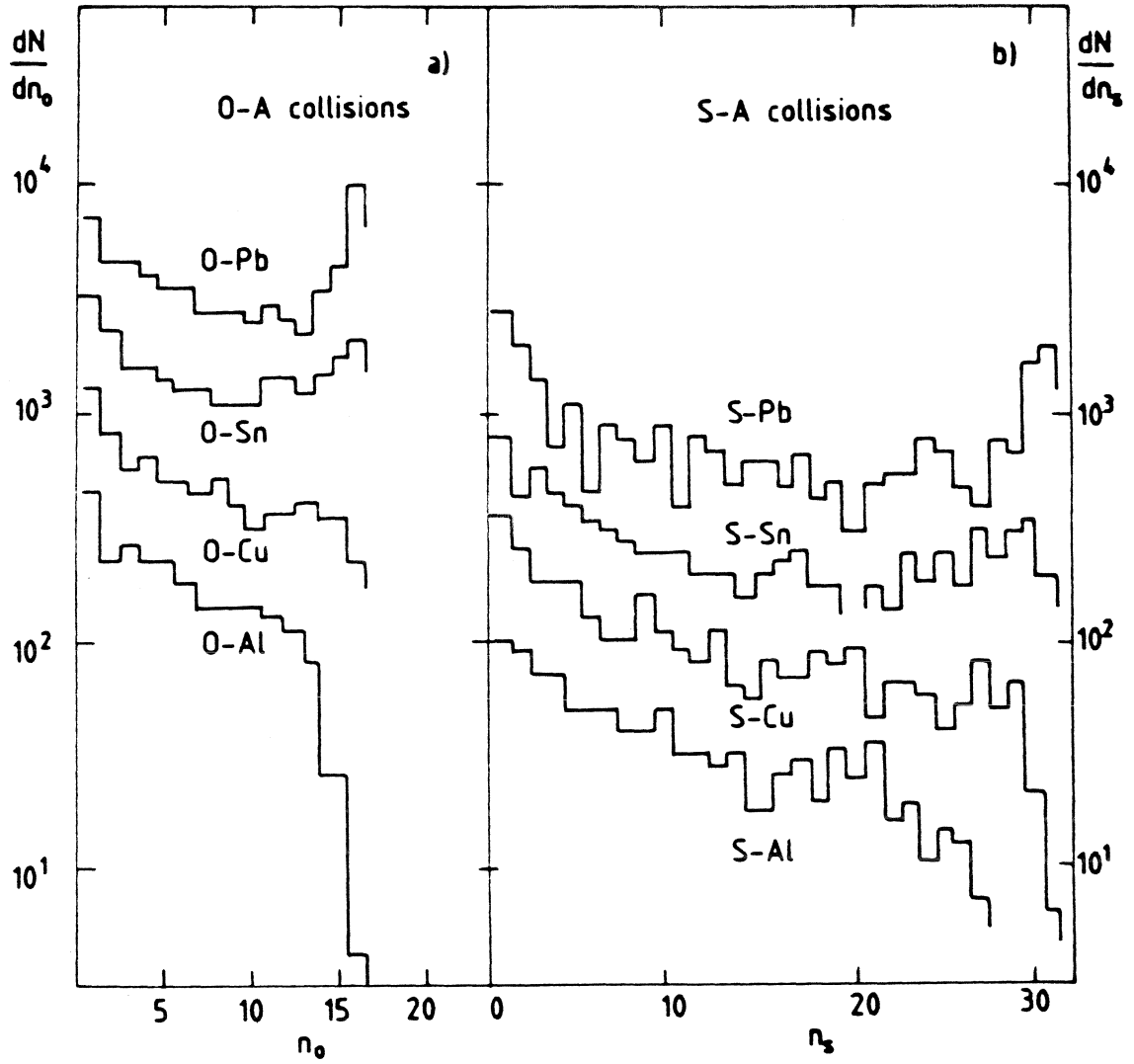


Fig. 2. Distributions in the number of projectile nucleons taking part in collisions of oxygen and sulfur ions with different nuclei. The peaks at  $n_0 = 16$  and  $n_s = 32$  correspond to central collisions. a) O-A collisions, b) S-A collisions.

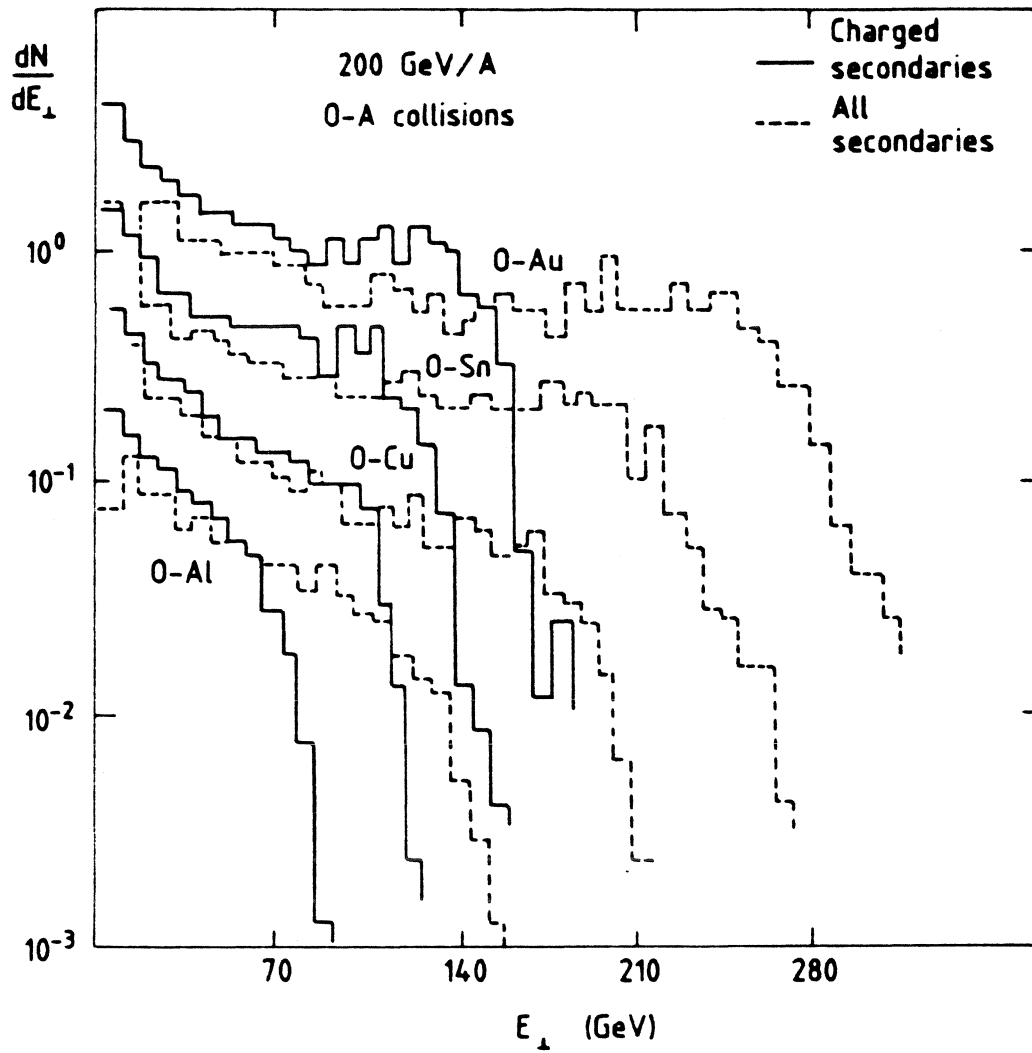


Fig. 3. Distributions of the transverse energy in oxygen-nucleus collisions at the energy of 200 GeV per nucleon. We give separately the transverse energy distribution for all secondaries and for charged secondaries.

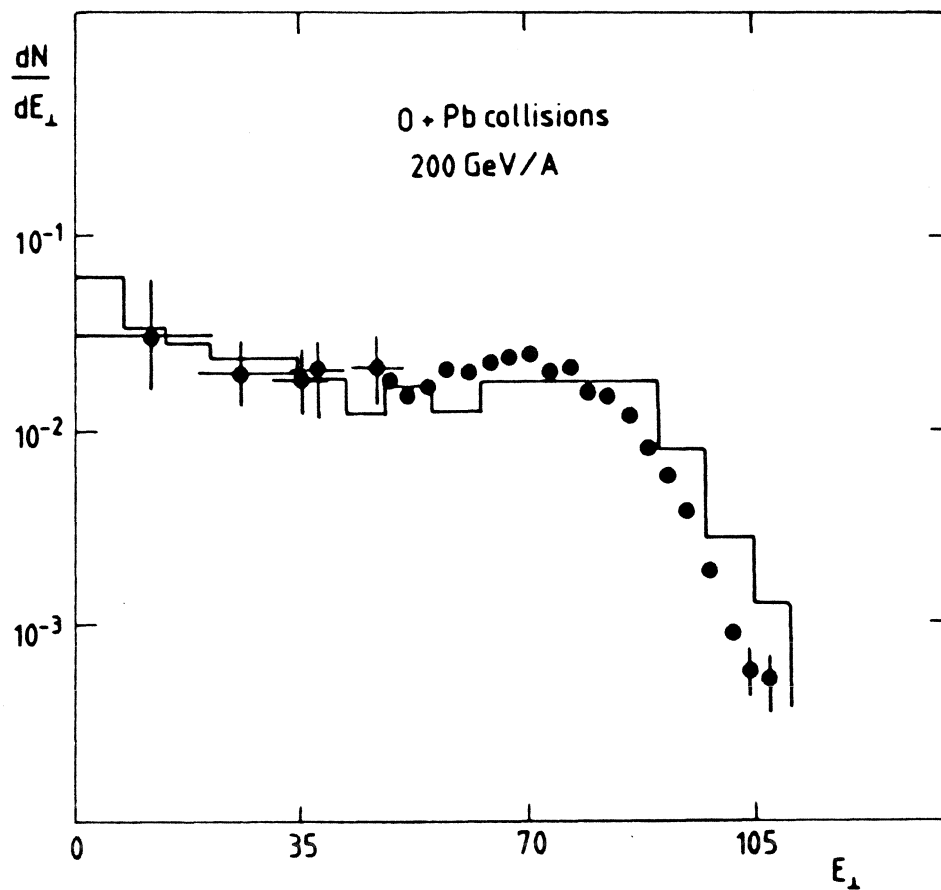


Fig. 4. The transverse energy distribution in oxygen-lead collisions with 200 GeV per nucleon. The results of the model (histogram) are compared with the experimental data (points) from the CERN SPS NA-35 Collaboration [2].